Accepted Manuscript

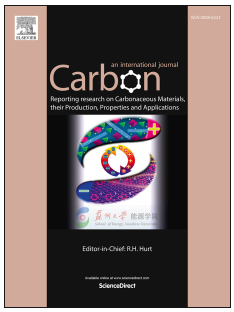

Exceptionally high performance of charged carbon nanotube arrays for CO_2 separation from flue gas

Lang Liu, David Nicholson, Suresh K. Bhatia

PII: S0008-6223(17)30925-9

DOI: 10.1016/j.carbon.2017.09.050

Reference: CARBON 12380

To appear in: *Carbon*

Received Date: 8 July 2017

Revised Date: 13 September 2017

Accepted Date: 14 September 2017

Please cite this article as: L. Liu, D. Nicholson, S.K. Bhatia, Exceptionally high performance of charged carbon nanotube arrays for CO_2 separation from flue gas, *Carbon* (2017), doi: 10.1016/j.carbon.2017.09.050.

Graphical Abstract

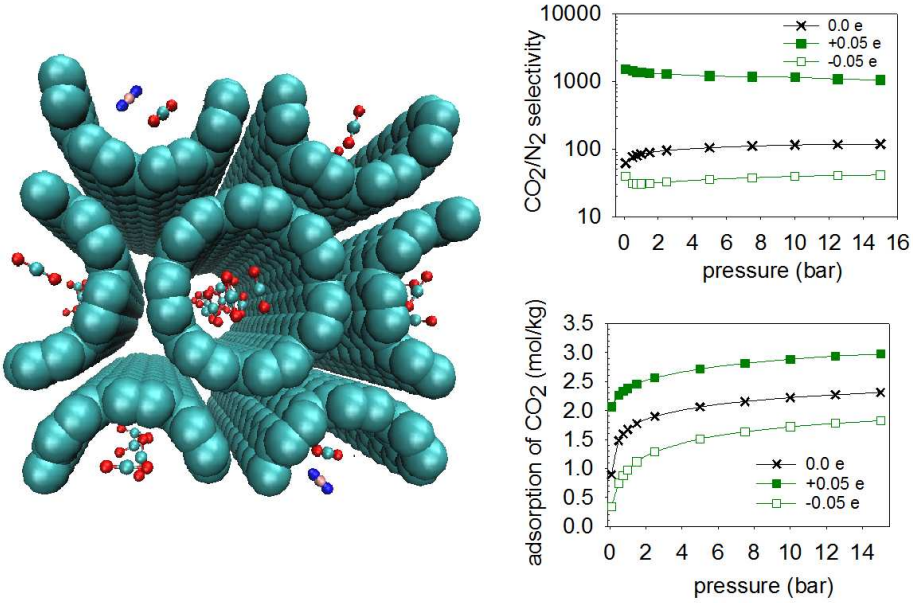

Exceptionally High Performance of Charged Carbon Nanotube Arrays for CO_2 Separation from Flue Gas

Lang Liu, David Nicholson and Suresh K. Bhatia*

School of Chemical Engineering, The University of Queensland Brisbane, QLD 4072, Australia

We use grand canonical Monte Carlo simulation to investigate the adsorption of a CO_2/N_2 mixture in neutral and charged (7, 7) carbon nanotube (CNT) arrays. It is found that both the adsorption of CO_2, and the CO_2/N_2 selectivity are either enhanced or reduced when the charges are positive or negative. The CO_2/N_2 selectivity in a CNT bundle carrying +0.05e charge with intertube distance of 0.335 nm exceeds 1000 for pressures up to 15 bar, which is remarkably high. It is seen that strong electrostatic interactions from neighbouring CNTs enhance the adsorption of CO_2 over N_2, and while the adsorption of CO_2 has complex dependence on intertube distance, the CO_2/N_2 selectivity decreases with intertube spacing. We propose a quantitative performance coefficient as an aid to assessing the efficiency of CNT bundles to separate CO_2 from flue gas, and show that a +0.05e charged bundle with intertube distance of 0.335 nm provides the best performance. Further, it is found that water vapor in flue gas imposes negligible effect on the adsorption of CO_2 and its selectivity over N_2 in the neutral and positively charged (7, 7) CNT bundles, but dramatically reduces the adsorption of CO_2 and N_2 in the negatively charged bundles.

*To whom correspondence may be addressed. Email: s.bhatia@uq.edu.au. Tel.: +61 7 3365 4263

1 Introduction

The anthropogenic gas, carbon dioxide (CO_2), is a major component of flue gas emitted from fossil fuel burning power plants, and has been identified as a major contributor to global warming and climate change [1, 2]. Post-combustion capture processes, that remove and permanently sequester CO_2 from flue gas streams, have been identified as a feasible solution to stabilize the atmospheric content of CO_2 [3, 4]. Among a wide range of possible post-combustion techniques [2], adsorptive separation of CO_2 has been recognised as an efficient process and has received extensive attention for its low energetic penalties. Bundles of single-walled carbon nanotubes (SWCNTs) [5] possess high specific surface area and strong host-adsorbate interaction [6], as well as near frictionless internal surfaces for transportation [7], making them one of the most promising adsorption materials for capturing CO_2 from flue gas. As indicated in our previous study [6] the (7, 7) SWCNT possesses both superior adsorption capacity for CO_2 and high CO_2/CH_4 selectivity at atmospheric pressure and ambient temperature, compared to amorphous carbons, activated carbon fiber-15 (ACF-15) and silicon carbide derived carbon (SiC-DC). Simulations by Kowalczyk et al. [8] have shown that the adsorption capacity of CO_2 in SWCNTs is a strong function of the CNT diameter, and that the adsorption capacity of CO_2 at 1.5 MPa, in tubes with optimum diameters, is higher than that in metal organic framework-177 (MOF-177) [9], which is considered to be amongst the most efficient nanoporous materials for CO_2 storage.

MOFs [10], zeolitic imidazolate frameworks (ZIFs) [11] and zeolites [12] have accessible metal and cationic sites, where electrostatic interactions between an adsorbate carrying a permanent multipole and the framework make an important contribution to the high adsorption and separation selectivity for the target species. In CNTs, however, electrostatic interactions with an adsorbate are negligible. For example Liu and Smit [11] found that removing the electrostatic interactions between the adsorbate and the framework reduced the adsorption of CO_2 and the CO_2/CH_4 and CO_2/N_2 selectivities by about 50% in ZIF-68 and ZIF-69. They also found that adsorption was enhanced for adsorbates with larger quadrupolar moments; accounting for the increase in selectivity for CO_2/N_2 and a decrease for CH_4/N_2 compared to selectivity in the same material without electrostatic interactions. CO_2, and N_2 have quadrupole moments of 13.4×10^{-40}, 4.7×10^{-40} Cm^2 respectively [13]. Therefore altering the charge distribution in CNTs should significantly affect the selectivity for CO_2 over N_2.

The electrical conductivity of CNTs indicates that they can be charged and discharged easily, which has already been exploited for electric swing adsorption (ESA) of CO_2, utilizing the direct Joule effect (resistance heating) to heat the adsorbent [3]. Both experiments and simulations [14, 15] have demonstrated that doping CNTs with an electron donor or acceptor, such as potassium or bromine, bestows a negative or positive charge, and that the magnitude of the charge can be as high as 0.1e per carbon atom. The charge that transfers to a carbon atom can be further adjusted by changing the ratio of dopant atoms to carbon atoms [16]. In addition, mounting the CNTs as the electrode of a capacitor [17], employing femtosecond layer pulses [18] or utilizing a charge injection method [19] provide alternative ways to charge the CNTs. In their simulation study, Deng et al. [16] reported that with a doping ratio of Li:C =1:3 in a (10, 10) hexagonal CNT bundle having an intertube distance of 0.9 nm, hydrogen adsorption was achieved as 6.0 wt% at 50 bar and room temperature; which is one order of magnitude higher than that in the neutral CNT bundle and only slightly below the DOE standard of 6.5 wt%. In the simulation study of Rahimi et al. [20], in which charges were assigned to each carbon atom in a bundle of 1.5 nm diameter single-walled carbon nanotubes, it was found that positive surface charge enhanced the adsorption of pure CO_2 by up to 35%, while negative charge suppressed adsorption. Conversely, Simonyan et al. [21] found that the adsorption of hydrogen was enhanced in negatively charged CNT bundles but suppressed in positively charged bundles.

In the studies cited above [16, 20, 21] although the effects of surface charge on adsorption of single species in CNT bundles are reported, the detailed mechanism has not been explicitly investigated. For instance, is it the surface charge on the CNT within which the adsorbed molecules lie that plays a major role in enhancing/suppressing the adsorption inside the CNT, or is it the surface charge on the neighbouring CNTs that plays a dominant role? Molecules with non-zero quadrupole moment, such as CO_2 and N_2, lose configurational freedom (i.e. entropy) to achieve the minimum potential energy configuration and adsorb into the charged CNT [20], while the additional adsorbate-CNT electrostatic interactions affect the adsorption energetically. It is critical to understand the cooperative effect between the entropic and energetic effects arising from the surface charge, as the adsorption generally shows opposite dependence on the positive and negative charges. In view of similar molecular configurations and non-zero quadrupole moments of CO_2 and N_2, it may be anticipated that the effect of surface charge on the CNT on the adsorption of pure component CO_2 and N_2 will be similar; however, no study of the effect of surface charge on the performance of CNT bundles in

separating CO_2 from flue gas (CO_2/N_2 mixture) has been made to date. Indeed, it is shown here that the mixture adsorption isotherms of CO_2 and N_2 (for mole ratio of CO_2/N_2=20/80 in the gas phase) demonstrate opposite dependence on the surface charge, and the CO_2/N_2 selectivity is dramatically enhanced/suppressed in positively/negatively charged bundles compared to the neutral bundle. Further, little is known about how the cooperative effect between the adsorbate-CNT (neutral and charged CNTs) interactions and the adsorbate-adsorbate interactions influences the dependence of CO_2/N_2 selectivity on the mixture pressure. The physical insights pertaining to these and other relevant issues are obtained in detail in this work. Since both adsorption capacity and selectivity determine the performance of the adsorbents, we propose a weight coefficient to assess the performance of charged CNT bundles in separating CO_2 from flue gas.

2 Simulation details

The adsorption of CO_2/N_2 mixtures in the neutral and charged (7, 7) CNT bundles has been investigated. Bundles of single-walled CNTs were arranged in a hexagonal lattice. The atomistic configuration of a unit cell comprising (7, 7) CNTs with an intertube distance of 0.5 nm is illustrated in Figures 1 (a) and (b). The intertube distance, δ, between two adjacent CNTs is defined by subtracting the diameter, d, of the CNT from the center to center distance, l, between these two CNTs. Here, $\delta = l - d$; the diameter, d =0.95 nm, of the (7, 7) CNT is defined as the center to center distance between two opposite carbon atoms of the CNT. The angles between three neighbouring CNTs were fixed at, 60^o. We varied the intertube distance of the hexagonal arrays from 0.335 to 1.5 nm to determine the optimized intertube distance. The dimensions, $L_x \times L_y \times L_z$, of the (7, 7) CNT arrays, with *z* in the axial direction, were $2.57 \times 4.45 \times 5.03$, $2.90 \times 2.52 \times 5.03$, $3.90 \times 3.38 \times 5.03$ and $4.90 \times 4.25 \times 5.03 \text{nm}^3$ respectively, corresponding to the intertube distances 0.335, 0.50, 1.0 and 1.5 nm.

The CNTs were treated as rigid structures with a Lennard-Jones (LJ) C-atom at each site, with $\sigma_C = 0.34$ nm, $\varepsilon_C / k_B = 28K$ [22]. In the charged bundles, charges of either 0.0, ± 0.01, ± 0.02 or ± 0.05 e, were placed on each carbon atom. The CO_2 was modelled by the EPM2 linear model of Harris and Yung [23] with 3 LJ sites and a quadrupole represented explicitly by point charges on each atom. Nitrogen was modelled by two LJ nitrogen atoms each carrying a negative charge, with a balancing positive charge located at the center of

mass of the molecule [24].The parameters of the CNT, CO_2 and N_2 are given in Table 1. The potential energy of interaction between individual atoms is expressed as a sum of LJ and electrostatic terms by:

$$u_{ij}^{(\alpha,\beta)} = 4\varepsilon_{ij}^{(\alpha,\beta)}\left[\left(\frac{\sigma_{ij}^{(\alpha,\beta)}}{r_{ij}^{(\alpha,\beta)}}\right)^{12} - \left(\frac{\sigma_{ij}^{(\alpha,\beta)}}{r_{ij}^{(\alpha,\beta)}}\right)^{6}\right] + \frac{1}{4\pi\varepsilon_0}\frac{q_i^{\alpha} q_j^{\beta}}{r_{ij}^{(\alpha,\beta)}} \quad (1)$$

where the first term on the right hand side represents the dispersive and Pauli overlap repulsive interactions, and the second term corresponds to the electrostatic interactions. $r_{ij}^{(\alpha,\beta)}$ is the distance between two sites *i* and *j* on molecules α and β, and q_i^{α} and q_j^{β} are the partial charges on sites *i* and *j* of molecules α and β. ε_0 is the permittivity of free space. The cross parameters were estimated using the Lorentz-Berthelot combining rules [25].

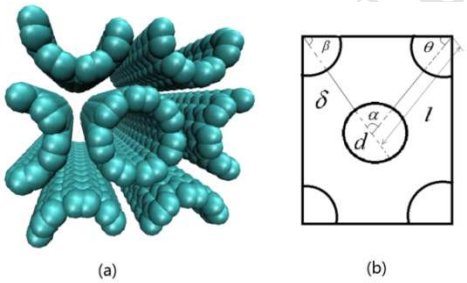

Figure 1. (a) Atomistic configuration of the (7, 7) CNT bundle with an intertube distance of 0.5 nm. (b) Schematic view of the elementary unit cell of the CNT bundles.

GCMC simulations were used to study the adsorption of CO_2/N_2 mixtures in CNT bundles, at 300 K, with a total pressure of up to 15 bar. Periodic boundary conditions were applied in all directions. A cut-off of 1.2 nm was applied to the LJ potential, and Ewald summations were used to correct the long range electrostatic interactions with a cut-off of 1.2 nm in real space. As the electrostatic interactions between the carbon atoms in the CNT are neglected, and individual fluid molecules are electrically neutral, the fluid-fluid and the fluid-charged CNT electrostatic interactions converge at infinite distance. Therefore, applying the Ewald summation method to correct the long range electrostatic interactions throughout our simulations is justified.

The CO_2/N_2 mole ratio in the gas phase was set as 20/80, similar to that in flue gases. The corresponding individual fugacities used in the simulations were determined from the Kunz and Wagner [26] natural gas equation of state. To obtain the isotherm, simulations were run

for at least 6.0×10^5 cycles (each cycle having N configurations, where N is the amount of molecules adsorbed, with minimum of 20), with the first 1×10^5 cycles used for equilibration. In addition, since flue gases are generally saturated with water, we also investigated the adsorption of a $CO_2/N_2/H_2O$ ternary mixture saturated with water (bulk composition is CO_2:N_2=20:80 with H_2O at its saturation pressure, 3.537 kPa at 300 K) in neutral and charged (7, 7) CNT bundles with the intertube separation of 0.335 nm. The SPC model was used to describe the water-adsorbate and water-CNT interactions, with the parameters of SPC model given in Table 1. The GCMC simulations for the ternary mixture saturated with water were extended to at least 1.5×10^7 cycles with the first 5×10^6 for the equilibration.

It is found in our simulations for the (6, 6) (diameter = 0.81 nm) and (10, 10) (diameter =1.356 nm) CNT bundles, both neutral and charged (+0.05e), with an intertube distance of 0.335 nm, that the adsorption capacity and the separation selectivity for CO_2 are both lower than in the corresponding (7, 7) bundles, at 1.0 bar and 300 K. In what follows, we therefore focus on the (7, 7) CNT bundles, as either decreasing or increasing the diameter of the (neutral or charged) CNT reduces the performance in separating CO_2 from flue gas.

Table 1. Lennard–Jones parameters, partial charges, configurational parameters and quadrupole moments for the CNT, CO_2 and N_2 and H_2O.

Molecule	atom	LJ parameters		Molecular model			Charge (e)	quadrupole moment (Cm^2)
		ε / k_B (K)	σ (nm)	X (nm)	Y (nm)	Z (nm)		
CNT	C	28.0	0.34					
CO_2	C	28.129	0.2757	0.0	0.0	0.0	0.6512	13.4×10^{-40} [13]
	O	80.507	0.3033	±0.1149	0.0	0.0	-0.3256	
N_2	N	36.0	0.331	±0.055	0.0	0.0	-0.482	4.7×10^{-40} [13]
	COM	0.0	0.0	0.0	0.0	0.0	0.964	
H_2O	H	0.0	0.0	±0.081649	0.05773	0.0	0.41	
	O	78.205	0.3166	0.0	0.0	0.0	-0.82	

3 Results and analysis

3.1 Effect of charge on the adsorption of CO_2/N_2 mixtures

Figures 2(a) and (b) show the adsorption isotherms for CO_2 and N_2 in neutral and charged (7, 7) CNT bundles with 0.335 nm intertube distance at 300 K. The CO_2/N_2 mole ratio in the gas phase is 20/80. At pressures below 15 bar, adsorption only occurs inside the nanotubes, because the intertube spacing is too narrow to admit N_2 or CO_2. It is seen that CO_2 is always preferentially adsorbed in the neutral and charged CNTs over N_2 as a consequence of stronger

affinity with the carbon wall [27] and larger quadrupole moment than the N_2. Nevertheless, the isotherms of CO_2 and N_2 show different dependencies on the sign of the surface charge. While increasing the positive or negative charge enhances or suppresses the adsorption capacity of CO_2, N_2 shows the opposite trend. For example, at 1.0 bar, when the surface charge is increased from 0.0 to +0.05e, the amount of CO_2 adsorbed increases from 1.67 to 2.38 mol/kg while the amount of N_2 adsorbed decreases from 0.08 to 0.007 mol/kg. As will be subsequently discussed, the significant enhancement in the adsorption of CO_2 in the positively charged CNT bundles is due to the additional CO_2-CNT coulomb interactions, and the reduction in the adsorption of N_2 is a consequence of the competitive adsorption between CO_2 and N_2. On the other hand, the reduction in the adsorption of CO_2 in the negatively charged CNT bundles is a result of losses in the available adsorption volume and the entropy, while the enhancement in the adsorption of N_2 is due to enhanced adsorption space left by CO_2 and smaller loss in configurational freedom compared to that for CO_2. A similar trend was found in neutral graphitic slit pores and the influence of rotational hindrance was also noted [28].

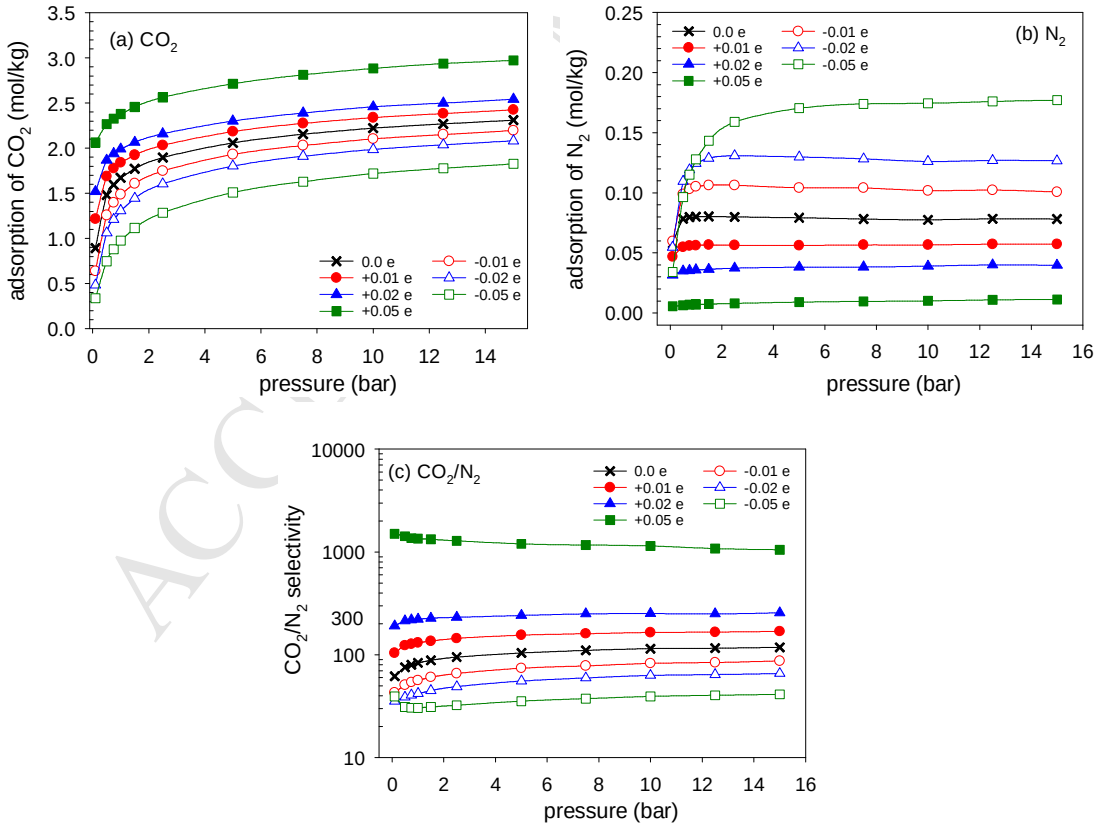

Figure 2. Adsorption isotherms at 300 K, of (a) CO_2, and (b) N_2. (c) CO_2/N_2 selectivity in neutral and charged (7, 7) CNT bundles with intertube separation of 0.335 nm. The CO_2/N_2 mole ratio in the gas phase is 20/80.

The equilibrium selectivity is defined as $(x_i / y_i)/(x_j / y_j)$, where x_i and y_i are the mole fractions of component *i* in the adsorbed phase and gas phase [6]. Since the adsorption of CO_2 is enhanced in the presence of a positive charge and that of N_2 diminished, the CO_2/N_2 selectivity is dramatically improved, compared to the negatively charged or neutral arrays. As shown in Figure 2(c), the equilibrium CO_2/N_2 selectivity increases or decreases when the applied charge is positive or negative compared to that in the neutral CNT. The CO_2/N_2 selectivity exceeds 1000 in the (7, 7) CNT bundle carrying a charge of +0.05e at pressures up to 15 bar, and reaches a value of 1348 at atmospheric pressure and ambient temperature. Table 2 lists the CO_2/N_2 selectivity in 22 other adsorbents studied in the literature [10, 11, 31-38], including MOFs, ZIFs, zeolites and activated carbons. The selectivity of CO_2/N_2 in the +0.05e charged (7, 7) CNT bundle with an intertube distance of 0.335 nm at 1.0 bar and ambient temperature is superior compared to all the other materials reviewed. For example, the CO_2/N_2 selectivity in the +0.05e charged (7, 7) CNT bundle is more than twice of that in metal-organic framework (rho-ZMOF), which has been identified as a promising material for flue gas separation due to its unprecedentedly high CO_2/N_2 selectivity [10]. It is interesting to note that the selectivity of CO_2/N_2 generally increases with pressure, except in the bundle with surface charge of +0.05e, in which the CO_2/N_2 selectivity decreases with pressure. The high selectivity performance of the charged CNTs studied here is highlighted by comparing them with other carbon adsorbents; for example, at a pressure of 1.0 bar the amount adsorbed in the charged nanotube is 2.38 mol/kg compared to 0.58 mol/kg and 0.42 mol/kg in neutral ACF-15 [29] and SiC-DC [30] respectively.

Since activated carbons can also be charged, we have investigated the potential of charged CNT bundles relative to the charged amorphous activated carbons. Figure S1 depicts the adsorption isotherms of components, CO_2 and N_2 (bulk composition is 20/80), and the CO_2/N_2 selectivity in the neutral and ±0.05e charged SiC-DC [6, 30], at 300 K. The LJ parameters of SiC-DC are $\varepsilon_C = 28.0$ K and $\delta_C = 3.4$ nm. Attributed to the enhanced adsorption volume in SiC-DC, the adsorption of CO_2 in +0.05e charged SiC-DC becomes higher than that in the +0.05e charged (7, 7) CNT bundle with the intertube separation of 0.335 nm when the pressure is above 0.75 bar at 300 K. On the other hand, the amounts of CO_2 adsorbed in the neutral and -0.05e charged SiC-DC are generally lower than those in the corresponding (7, 7) CNT bundles except at the pressures above 10.0 bar. This is mainly a consequence of the reduced adsorbate-adsorbent interactions in the neutral and negatively

charged SiC-DC with respect to the counterparts in the (7, 7) CNT bundles [6]. The molecular configuration and pore size distribution of SiC-DC are depicted in Figure S1 (d) and the way of determining the pore size distribution was provided in our previous study [6]. Nevertheless, the CO_2/N_2 selectivities in the neutral and charged SiC-DC are always far below those in the corresponding (7, 7) CNT bundles. Measured with the comprehensive performance coefficient (λ_e, proposed in section 3.4), the performances of neutral and ±0.05e charged (7, 7) CNT bundles in separation CO_2 from flue gas are 6.2, 31.32 and 15.38 times better at 1.0 bar and 4.25, 10.27 and 2.62 times better at 15 bar, than the corresponding SiC-DCs. However, in the neutral and negatively charged SiC-DC, the adsorption of CO_2/N_2 is far away from saturation, such that the components, CO_2 and N_2, do not compete for the adsorption volume. Consequently, the adsorption of CO_2 and N_2 in SiC-DC are both reduced by the negative surface charge, which differs from that in the negatively charged (7, 7) CNT bundle with intertube separation of 0.335 nm, in which the adsorption of N_2 is enhanced by the negative surface charge as a result of reduced adsorption of CO_2 while gaining additional adsorption volume. Accordingly, the adsorption of N_2 is enhanced in the positively charged SiC-DC compared to that in the neutral SiC-DC when the pressure is low, which is mainly attributed to the N_2-SiC-DC additional coulomb interactions, and is reduced at high pressures as a result of competition between CO_2 and N_2 for the adsorption volume. Nevertheless, while the adsorption of CO_2 and N_2 are reduced in the negatively charged SiC-DC, the narrow pores become more relatively favourable for the adsorption of CO_2/N_2 mixture than in the neutral SiC-DC. It is expected that the effect of negative charge on reducing the adsorption is weaker in the narrow pores with respect to the large pores, which is because the LJ interactions are more prevalent than the electrostatic interactions in the narrow pores considering the LJ interaction scales as r^{-6} while the electrostatic interaction scales as r^{-1}. In addition, the diameter of CO_2 is smaller than that of N_2, as given in Table 1. Therefore CO_2 is able to occupy the narrow pores which are not accessible for the N_2. Consequently, this molecular sieving effect for CO_2 over N_2 is more prevalent in the negatively charged SiC-DC than in the neutral SiC-DC, and the CO_2/N_2selectivity is enhanced by the negative surface charge relative to that in the neutral SiC-DC when the pressure is low as the adsorption mainly occurs in the narrow pores, and is reduced after 15 bar as the adsorption shifts to the large pores. However, a more detailed and systematic study of the adsorption of CO_2/N_2 mixture in amorphous carbons is out of the scope of the current work.

Table 2. CO_2/N_2 selectivities in different nanoporous materials at 1.0 bar

Material	mole ratio of CO_2/N_2	Temp (K)	Selectivity	Reference
Cu-BTC	15.6/86.4	298	20	[31]
IRMOF-1	10/90	298	7	[32]
MOF-508b	50/50	303	4	[33]
roh-ZMOF	15/85	298	500	[10]
MgMOF-74	15/85	300	220	[34]
mmen-CuTTri	15/85	300	400	[34]
MOF-177	15/85	300	3.5	[34]
ZIF-68	15/85	298	14	[11]
ZIF-69	15/85	298	25	[11]
MFI	15/85	300	10	[34]
FAU-Si	15/85	300	6	[34]
Silicalite	10/90	308	30	[34]
ITQ-3	10/90	308	70	[35]
JBW	15/85	300	600	[34]
AFX	15/85	300	250	[34]
NaX	15/85	300	180	[34]
DDR	50/50	298	24	[36]
LTA	50/50	298	11	[36]
Na-4A	20/80	298	16.5	[37]
C168	21/79	300	180	[38]
ACF-15	20/80	300	13	This work
SiC-DC	20/80	300	11	This work

It was shown by Jiang and Sandler [38] in their simulation work that both the adsorption of pure CO_2 and the CO_2 selectivity for the CO_2/N_2 mixture (bulk composition is 0.21:0.79) in the C_{168} Schwarzite were significantly larger with the ab initio potential for the C_{168} than with the Steele potential for the C_{168}. This implies the adsorption and selectivity of CO_2 can be potentially enhanced in the case where the interaction of the adsorbate with the CNT is enhanced, such as in the multiwalled carbon nanotube bundles [39] or the CNT with dopants having stronger affinity. Figure 2 demonstrates that enhancing the the electrostatic interactions of the adsorbate with the positively charged CNT enhances the adsorption of CO_2 and CO_2/N_2 selectivity noticeably. Additionally, it is found both the adsorption and the selectivity of CO_2 in the neutral and positively charged CNT bundles increase significantly with the adsorbate-CNT LJ interactions, which is evident in Figures S2 (a) and (b). To reveal this, two alternative sets of the LJ parameters based on the Steele potential are considered for the CNT, which are $\varepsilon_C / k_B = 28.0 \times 0.8 = 22.4$ K , $\delta_C = 3.4$ nm and $\varepsilon_C / k_B = 28.0 \times 1.2 = 33.6$ K K, $\delta_C = 3.4$ nm. The adsorption isotherms of CO_2 and CO_2/N_2 selectivities in the neutral and +0.05e charged (7, 7) CNT bundles with different LJ

parameters are depicted in Figure S2. Moreover, it is interesting to note that the relative enhancements in the adsorption of CO_2 and the CO_2/N_2 selectivity in the positively charged CNT bundles relative to those in the neutral CNT bundles are reduced when the LJ interactions of the adsorbate with the CNT are enhanced, evident in Figures S2 (c) and (d). This is because the coulomb part of the adsorbate-CNT interactions makes smaller contribution to the overall interactions when the LJ component of the adsorbate-CNT interactions is more prevalent. In summary, both the adsorption and selectivity of CO_2 could be enhanced/reduced in the case where the adsorbate-adsorbent interactions are strengthened/weakened. It is shown that the performances of the neutral and charged CNT bundles in separating CO_2 from flue gas predicted in our simulations are actually sensitive to the force filed parameters used to capture the adsorbate-CNT interactions. In other words, the performance of the CNT bundle in separating CO_2 from flue gas could vary significantly when the CNT carries different dopants and structural defects [40-42].

3.2 Effect of charge on adsorbate molecular configurations

Figure 3 and Figure 4, show the orientation angle profiles and the radial density profiles at 1.0 bar, for CO_2 and N_2 in the (7, 7) CNT bundles carrying different charges. The corresponding orientation angle and radial density profiles at 15 bar are given in Figures S3 and S4, and show that similar configurations are found at both low and high pressures. The orientation angle, θ, is defined as the angle between the molecular axis and the axis of the CNT.

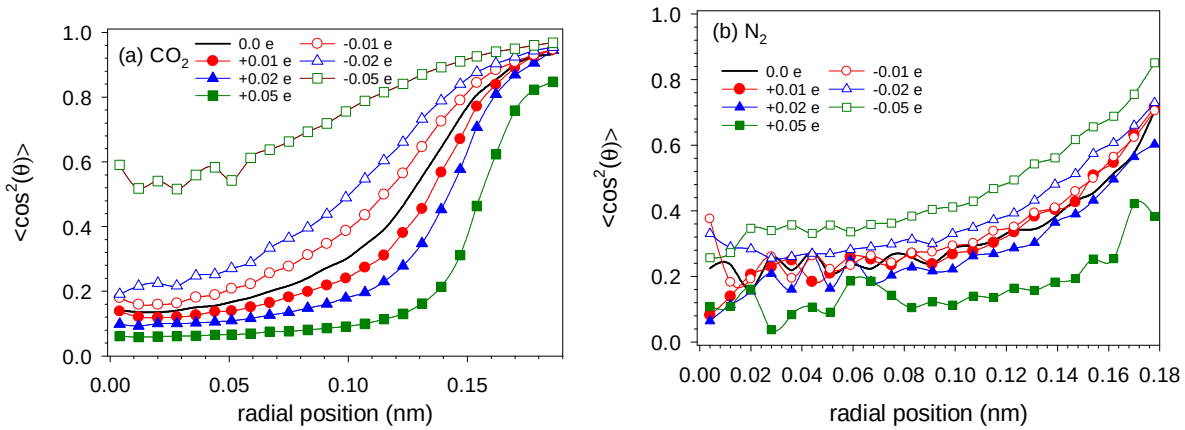

Figure 3. Orientation angle profiles, at 1.0 bar 300 K of (a) CO_2, and (b) N_2 in (7, 7) CNT bundles carrying different charges. The intertube separation is 0.335 nm.

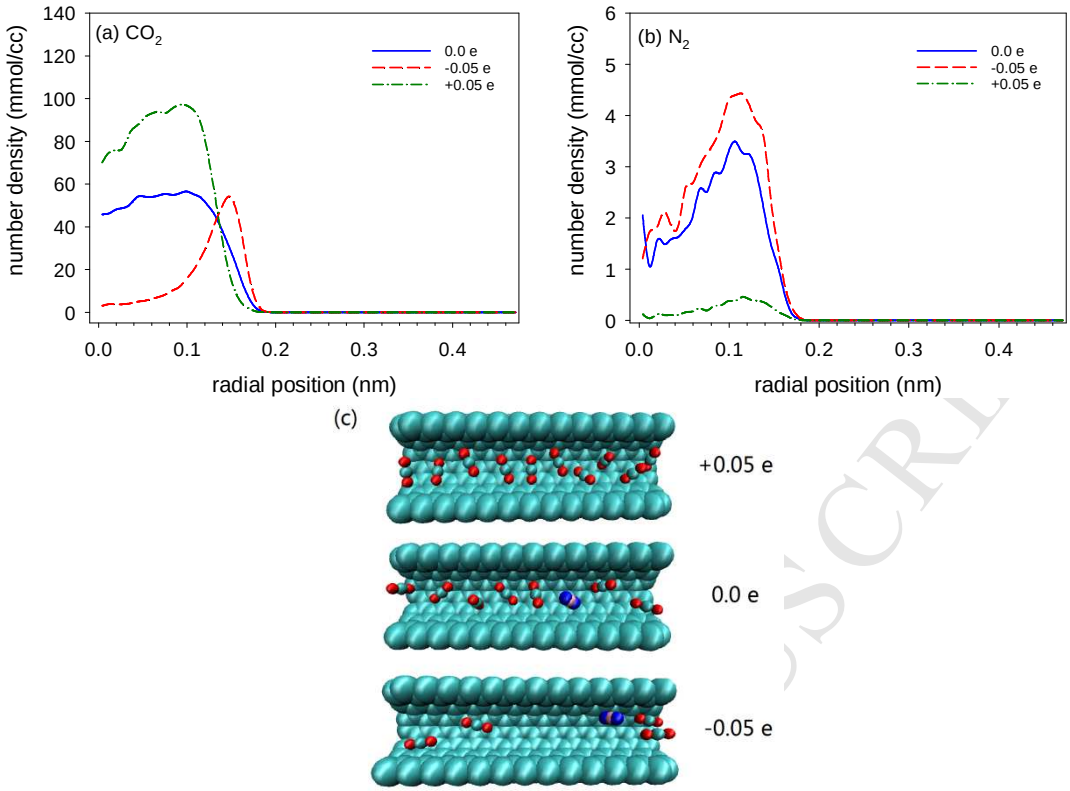

Figure 4. Radial density profiles at 1.0 bar and 300 K of (a) CO_2, and (b) N_2 inside a CNT in the (7, 7) CNT arrays carrying different charges. The intertube distance is 0.335 nm. (c) Snapshot of the configurations of CO_2/N_2 mixture inside a CNT in bundles carrying different charges, with half of the carbon wall being removed for visualization. The red and cyan spheres are the oxygen and carbon atoms of CO_2, and the blue and pink spheres are the nitrogen atom and center of mass of N_2.

As illustrated in Figures 3 (a) and (b), the orientation angles, both for CO_2 and N_2, increase with increasing positive charge or decrease with increasing negative charge. At the maxima in the CO_2 density profiles, the mean orientation angles of CO_2, $< \theta_{co_2} >$, are 17^0, 55^0 and 73^0 for surface charges of -0.05, 0.0 and +0.05 e. As the surface charge changes from negative to positive, the molecules tend to tilt away from the wall and to span the pore as the negatively charged atoms become more strongly attracted to the positive surface charges. Consequently, the radial position of the center of mass of the dominant component, CO_2, shifts towards the center of the CNT. The mean orientation angles for N_2 at the maxima in the density profiles are: $< \theta_{N_2} > = 44^0$, 54^0 and 67^0 for surface charges of -0.05e, 0.0e and +0.05e. When the surface charges are negative the energetically preferred orientation is parallel to the CNT axis, leading to larger footprint in the axial direction of the CNT and reduced entropy (configurational freedom) for CO_2 molecules compared to that in the neutral and positively charged CNT bundles, demonstrated in Figures 3(a) and 4(c) [28]. Since the remaining axial

space is too small to accommodate further adsorption of CO_2 in the negatively charged CNTs, a CO_2 molecule with larger orientation angle has a smaller footprint in the axial direction in the (7, 7) CNT, and can efficiently take up the space in the neutral and positively charged CNT bundles. The size of a CO_2 molecule is 0.5331 nm in the axial direction and is 0.3033 nm for the diameter. Additionally, the central space in the neutral and positively charged (7, 7) CNT becomes available for the adsorption of tilted CO_2 molecules, providing additional rotation and radial translocation freedom for the CO_2 molecules, i.e. enhanced entropy for the CO_2 molecules, compared to in the negatively charged CNT bundles, evident from Figures 4(a) and (c).

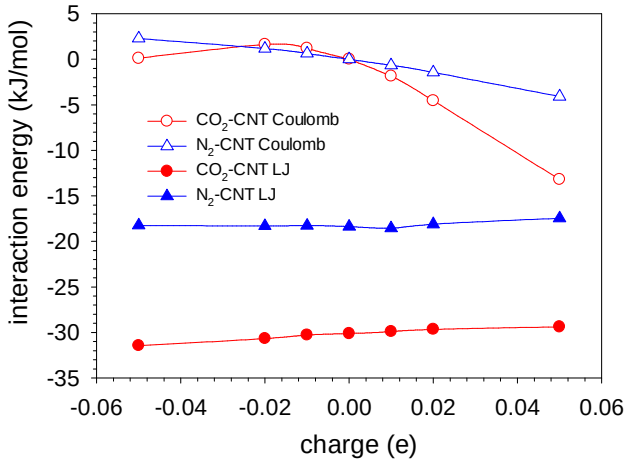

Figure 5. Variation of the LJ and electrostatic interactions versus the surface charge, at 1.0 bar and 300 K, for CO_2-CNT and N_2-CNT pairs in CNT bundles carrying different charges.

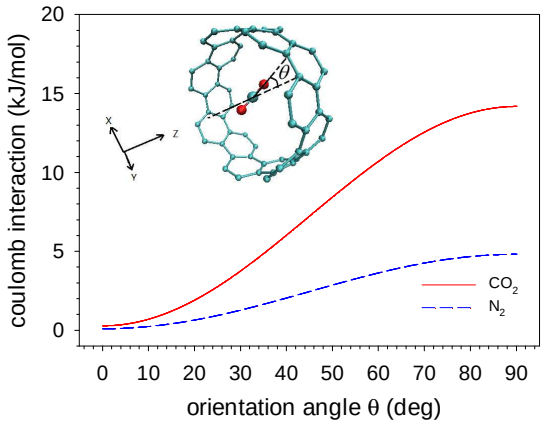

Figure 6. Variation of the CO_2-CNT and N_2-CNT electrostatic interactions with orientation angle in the (7, 7) CNT bundle carrying -0.05e charge. The molecules are fixed at positions $r =$ 0.0384 and 0.0845 nm for CO_2 and N_2 respectively, with $r = 0$ being the center of the central tube of the CNT bundle. A schematic of the CO_2 molecule located at the center of a unit cell of the single (7, 7) CNT is provided for visualization.

The ensemble averaged adsorbate-CNT interactions were determined by averaging over the interactions for all the molecules of a given species. Figure 5 shows that the LJ interactions

for CO_2-CNT and N_2-CNT are always attractive, and almost invariant when the surface charge is changed from -0.05e to +0.05e. The slight decrease in the CO_2-CNT LJ interactions occurs because the CO_2 molecules shift slightly, away from the potential energy minimum at the wall (Figure 4(a)). However, the electrostatic interactions between CO_2 or N_2 and the nanotube both vary strongly with the change in the surface charge; especially when the charge is positive. The LJ interactions therefore have negligible influence on the molecular configuration of the adsorbate.

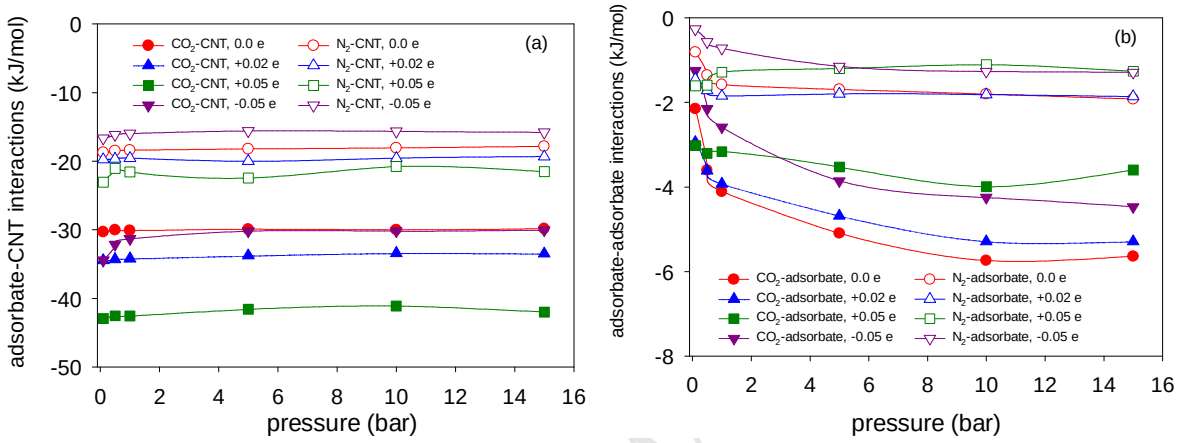

Figure 7. Variation of the interaction energies including the LJ and electrostatic components with pressure at 300 K, in (7, 7) CNT arrays carrying different charges. The intertube distance is 0.335 nm. (a) Adsorbate-CNT, and (b) adsorbate-adsorbate interactions.

When the CO_2 and N_2 molecules are aligned parallel to the axis of the negatively charged CNT, increasing the surface charge strengthens the repulsive adsorbate-CNT electrostatic interactions, as demonstrated in Figure 5. Calculations of the electrostatic interaction for a single molecule located in the central tube of the CNT bundle carrying charges of -0.05e with the whole bundle, show that the repulsive interaction decreases with the orientation angle and tends to diminish at the orientation angle $\theta = 0^0$, evident in Figure 6. In this calculation, the radial positions for the centres of mass (COMs) were fixed at $r_{p,CO_2} = r - \sigma_{C-O} - l_{C-O} = 0.0384$ nm and $r_{p,N_2} = r - \sigma_{C-N} - l_{N-M} = 0.0845$ nm, where σ_{C-O} and σ_{C-N} are the LJ diameters between the carbon atom in the CNT and the oxygen in the CO_2 or the nitrogen in the N_2, l_{C-O} (=0.149 nm) is the C=O bond length and l_{N-M} (=0.055 nm) is the distance between the COM and a N atom, and $r_p = 0.0$ denotes the center of the central tube of the CNT bundle. As shown in Figure 3 (a), when the magnitude of the negative surface charge increases from 0.0 to -0.02e, the ensemble averaged orientation angle of CO_2, $\langle \theta_{CO_2} \rangle$

decreases, so increasing the magnitude of the negative charge overrides the decrease in repulsion due to reduction in the orientation angle. However, when the magnitude of the surface charge further increases to -0.05e, the reduction in the repulsion due to reduced orientation angle dominates over the effect of increasing the magnitude of the negative charge. Consequently, the repulsion arising from the CO_2-CNT electrostatic interactions reduces. The N_2-CNT electrostatic interactions have a much weaker dependence on the orientation angle because of its weaker quadrupole, and, hence, the repulsive N_2-CNT electrostatic interaction always increases with the magnitude of the negative charge. Since the CO_2-CNT interactions vary only slightly with increased negative charge, but the orientation angle and the entropy of CO_2 are noticeably reduced, it may be concluded that this reductions in the orientation angle (i.e. enlarged footprint in the axial direction of the CNT) and the associated configurational freedom of CO_2 mainly account for the reduced adsorption of CO_2 in the negatively charged (7, 7) CNT arrays.

From Figures 5 and 6 it is confirmed that the parallel orientation is the most energetically favourable configuration for the adsorption of CO_2 and N_2 in the negatively charged CNT bundles. Regarding this, a single nitrogen molecule can occupy a given axial location that is not available for a parallel orientated CO_2 molecule leaving ample space for N_2. Due to the reduction in the adsorption of CO_2 and the enhanced fraction of adsorption space for N_2, the amount of N_2 adsorbed is enhanced by a negatively charged surface. In addition, Figure 6 also emphasises the fact that the entropy loss due to constraining the orientation angle of the adsorbate to achieve the energetically preferred configuration in the negatively charged CNT bundles is much weaker for the N_2 molecule than for the CO_2 molecule. In other words, there is a higher configurational freedom for the N_2 to adsorb in the negatively charged CNT bundle in comparison to the CO_2. Consequently, the CO_2/N_2 selectivity is reduced by a negatively charged surface. Nevertheless, increasing the positive charge increases the orientation angles of CO_2 and N_2 as well as the adsorbate-CNT electrostatic interactions for both components. When the surface is positive, CO_2 molecules have greater tendency to span towards the center of the pore and distribute vertically inside the CNT, compared to the neutral and negatively charged bundles, evident from Figures 3 (a) and 4 (a) and Figures S3(a) and S4(a). Although there is entropy loss for CO_2 molecules in the positively charged bundles compared to that in the neutral CNT bundles, the vertical molecular configuration of CO_2 molecules renders smaller footprint for CO_2 in the axial direction of the CNT and facilitates tighter packing, evident from Figures 3(a) and 4 (a) and (c). Moreover, there are significant

additional adsorbate-CNT electrostatic interactions in the positively charged bundles, and the CO_2-CNT electrostatic interactions are much greater and increase more rapidly with the surface charge than the weaker N_2 (see Table 1), as the quadruple moment of CO_2 is more significant than that of N_2 [13]. As a consequence, increasing the positive charge prompts the adsorption of CO_2 while dramatically reducing the adsorption of N_2 due to the significant loss in the available adsorption volume for N_2. This effect achieves a maximum at the surface charge of +0.05e, at which CO_2 molecules distribute almost vertically in the CNT and experiences the strong CO_2-CNT attractive interactions. In brief, the enhanced adsorption of CO_2 and the CO_2/N_2 selectivity in the positively charged CNTs is a consequence of the additional CO_2-CNT coulomb interactions and the tightly packing of vertically distributed CO_2 molecules in the CNT.

The pressure dependence of the interaction energies including the LJ and electrostatic components is shown in Figure 7, in which the ensemble averaged adsorbate-adsorbate interaction is defined as the summation of the interactions of the target species with themselves and with the other species. While the adsorbate-CNT (CO_2-CNT and N_2-CNT) interactions including the LJ and electrostatic parts vary very little with pressure, there is a stronger dependence of the adsorbate-adsorbate energy. When the CNT arrays are neutral or negatively charged, the CO_2-adsorbate and N_2-adsorbate interactions both increase quite strongly with pressure; the CO_2-adsorbate interactions being much greater and increasing more rapidly than the N_2 interactions. Consequently, the adsorbate-adsorbate interactions further facilitate the adsorption of CO_2 over N_2 at high pressures, and the CO_2/N_2 selectivity increases with pressure in the neutral and negatively charged CNT arrays. Similarly, the CO_2/N_2 selectivity increases with pressure in the positively charged CNT arrays when the surface charge is below +0.02e, as is evident from Figure 7. However, at the surface charge of +0.05e, the adsorption of CO_2 approaches saturation at very low pressure, such that increasing the pressure enhances the adsorption of CO_2 by further packing the vertically distributed CO_2 molecules, and the CO_2-adsorbate interactions subsequently increase only slightly with pressure below 10 bar and decrease after that. Since the available adsorption space left for N_2 is not further reduced noticeably by CO_2 with increase in pressure as the adsorption of CO_2 occurs mainly by tighter packing, the N_2 molecule has greater chance to adsorb into the fraction of space that is not available at low pressure. As a consequence, the CO_2/N_2 selectivity decreases with increase in pressure, when the surface charge on the (7, 7) CNT array reaches +0.05e.

It is seen in Figure 7(b) that when the pressure is below 0.5 bar and the adsorption of CO_2/N_2 mixture is far away from saturation, the CO_2-adsorbate interactions increase with increasing positive charge and are stronger than those in the neutral CNT bundle. However, as the pressure increases, the adsorption of the CO_2/N_2 mixture in the positively charged bundles approaches saturation more quickly compared to that in the neutral bundle, so that the adsorbate experiences dramatically enhanced repulsive interactions from the nearest neighbours and weakly enhanced attractive interactions from the distant adsorbate molecules. In such case, while the adsorption of CO_2 increases with the positive surface charge via tighter packing, the CO_2-adsorbate interactions conversely decrease with increasing positive charge, and are generally weaker than those in the neutral bundles. The reason for the weaker adsorbate-adsorbate interactions in the negatively charged bundles is mainly attributed to the weak adsorption of CO_2/N_2 mixture, in comparison to neutral bundles.

3.3 Effect of intertube distance on the adsorption of CO_2/N_2 mixture

The adsorption isotherms of CO_2 and N_2 for the CO_2/N_2 binary mixture (with a mole ratio of 20:80 in the gas phase) and the CO_2/N_2 selectivities at 300 K, in the (+0.05e) positively charged (7, 7) CNT arrays with intertube distances ranging from 0.335 to 1.5 nm, are depicted in Figure 8. The adsorption capacities can be either enhanced or reduced with increase in the intertube distance, but the CO_2/N_2 selectivity is reduced monotonically. Specifically, the CO_2/N_2 selectivity reduces from 1348 to 33.3, more than one order of magnitude, as the intertube distance increases from 0.335 to 1.5 nm at 1.0 bar and 300 K. This is because increasing the intertube distance provides additional volume but weakens the adsorbate-CNT interactions. The adsorption of CO_2/N_2 mixture in CNT bundles is therefore determined by the competition between the additionally available adsorption volume in the interspace and the reduced adsorbate-CNT interactions. However, since the adsorbate-CNT interactions decrease with intertube distance more rapidly for the CO_2-CNT case than for N_2-CNT, increasing the intertube distance reduces the CO_2/N_2 selectivity in the positively charged CNT bundles. Figure 9 depicts the overall interaction energies including the LJ and the coulomb components of adsorbate (CO_2 and N_2) with the CNT for the adsorbate inside and outside the CNT in the bundles with the intertube distances ranging from 0.335 to 1.5 nm, at 1.0 bar and 300 K. Similar adsorbate-CNT interactions are observed for the adsorbate inside and outside the CNT at high pressures. A snapshot of the configurations of the CO_2/N_2 mixture adsorbed in the (7, 7) CNT bundle carrying +0.05e charge with intertube distances of 0.335, 0.5, 1.0 and 1.5 nm, at 1.0 bar and 300 K are shown in Figure S5.

At the low pressures below 1.0 bar, the maximum adsorption of CO_2 is always achieved in the CNT bundle with an intertube distance of 0.5 nm, because in this case the interactions outside the tubes are almost as strong as those inside the tube and are comparable to those inside the tube of the CNT bundle with $\delta = 0.335$ nm, as shown in Figure 9. Consequently, the amounts of CO_2 adsorbed inside and outside the CNT are almost equal, observed in our simulations. Due to the additional adsorption space outside the tube, the adsorption of N_2 is also enhanced in the bundle with intertube distance $\delta = 0.5$ nm, compared to that in the bundle with $\delta = 0.335$ nm.

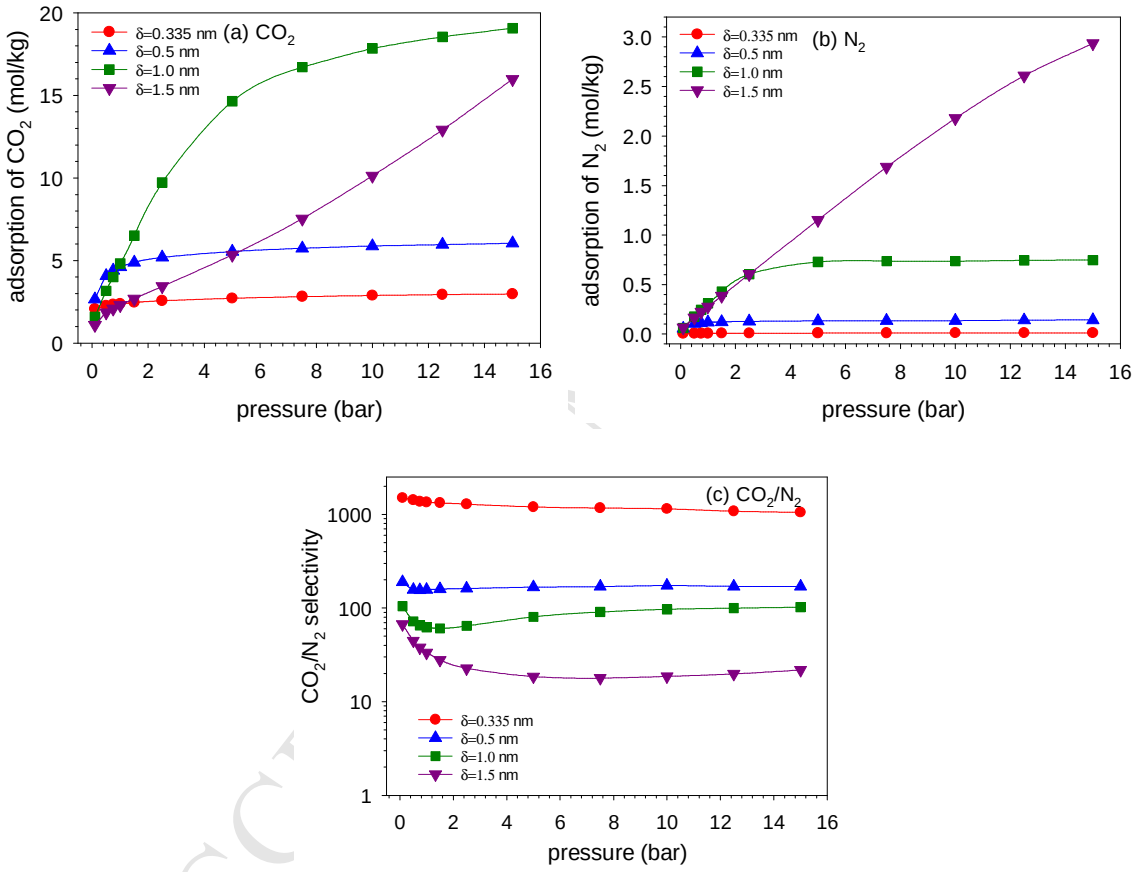

Figure 8. Adsorption isotherms at 300 K in the +0.05e charged (7, 7) CNT arrays with intertube separations ranging from 0.335 to 1.5 nm. (a) CO_2, and (b) N_2. (c) Variation of the CO_2/N_2 selectivity with pressure. The mole ratio of CO_2/N_2 is 20/80 in the gas phase.

At the intertube distance of 1.0 nm, although there is more adsorption space the CNT interaction with the adsorbates is weaker. However, the adsorption of CO_2 is still significantly higher than that in the bundle with $\delta = 0.335$ nm due to the significantly enhanced adsorption volume. As a consequence of reducing the adsorbate-CNT interactions the adsorption of N_2 becomes more prevalent, and the CO_2/N_2 selectivity is reduced.

Moreover due to the additional adsorption space and moderate N_2-CNT interactions, the adsorption of N_2 achieves its maximum in the bundle with $\delta = 1.0$ nm at low pressures, among all the +0.05e charged CNT bundles considered. The minimum adsorption of CO_2 and the second highest adsorption of N_2 in the low pressure regime were observed in the bundle with $\delta = 1.5$ nm.

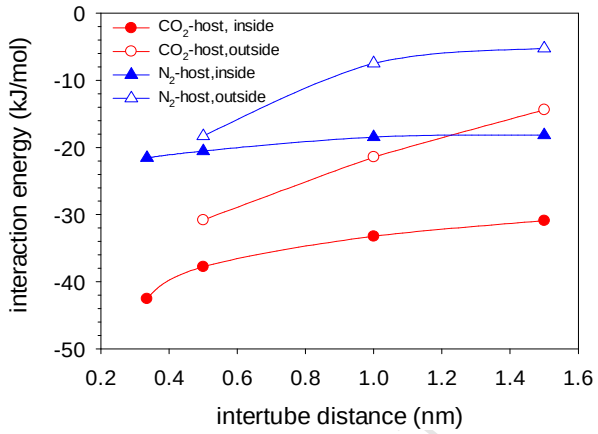

Figure 9. Variation of the overall interactions at 1.0 bar and 300 K with +0.05e-charged (7,7) CNT arrays, for CO_2 and N_2, for adsorbate located inside a CNT, or in the intertube space.

At higher pressures, while the adsorption of CO_2 and N_2 approach saturation in the CNT bundles with intertube distances of 0.335, 0.5 and 1.0 nm, it increases rapidly in bundles with larger intertube distance due to the additional adsorption space in the intertube space. Since the adsorbate-CNT interactions are much weaker in the bundle with $\delta = 1.5$ nm than those in the bundle with $\delta = 1.0$ nm, the CO_2 selectivity is lower. However, as a balance between the adsorption volume and the adsorbate-CNT interactions, the maximum adsorption of CO_2 is achieved in the bundle with $\delta = 1.0$ nm. Eventually, the cross interactions (including the LJ and coulomb parts) between the adsorbate molecules inside and outside the CNT have negligible effect on the adsorption of CO_2/N_2 mixture inside and outside the CNTs. In our GCMC simulations, we calculated the ensemble averaged interactions of each adsorbate species located inside/outside the CNT with the adsorbate (CO_2+N_2) located outside/inside the CNT. The estimated ratios of the interactions between the internal/external adsorbate species and the external/internal adsorbate (CO_2+N_2) to the interactions of the internal/external adsorbate species with host in the +0.05e charged (7, 7) CNT bundles with different intertube distances are depicted in Figure S6. It is seen, both at the low and high pressures, the cross interactions are negligible compared to the corresponding adsorbate-CNT

interactions. In addition, the same trends are observed in the neutral and negatively charged (7, 7) CNT bundles.

The interspace formed by neighbouring CNTs is the interstitial channel among three neighbouring CNTs and the groove space between two opposite CNT surfaces. Intriguingly, as the intertube distance increases, the most favorable space for the adsorption of CO_2 outside the CNT shifts from the interstices to the groove space, leaving the interstices as most unfavourable space for the adsorption. Figure 10 shows the density distributions of CO_2 in positively charged (7, 7) CNT arrays, for intertube distances ranging from 0.5 to 1.5 nm, at 10 bar. When the intertube distance is increased to 0.5 nm, adsorption of the CO_2/N_2 mixture outside the CNT only occurs in the interstices. However, when the intertube distance increases beyond that, CO_2 adsorbs at the external surfaces with a higher adsorbate density in the groove space. For instance, at the intertube distance of 1.0 nm, two adsorbed layers are observed in the grooves at 10 bar. One can expect that, at the low pressure, the adsorption of adsorbate preferentially occurs in the positions at which the adsorbate-CNT interactions are strongest. In this regard, Figure 9 also reveals the fact that the internal space in the positively charged (7, 7) CNT arrays is always more energetically favorable for the adsorption of CO_2 compared to the interstice and the groove space. This conclusion generally applies in the neutral and negatively charged bundles as well, with the exception of the -0.05e charged bundle with $\delta = 0.5$ nm, in which the interactions of adsorbate-CNT for adsorbate inside the CNT are slightly lower than those in the interstices.

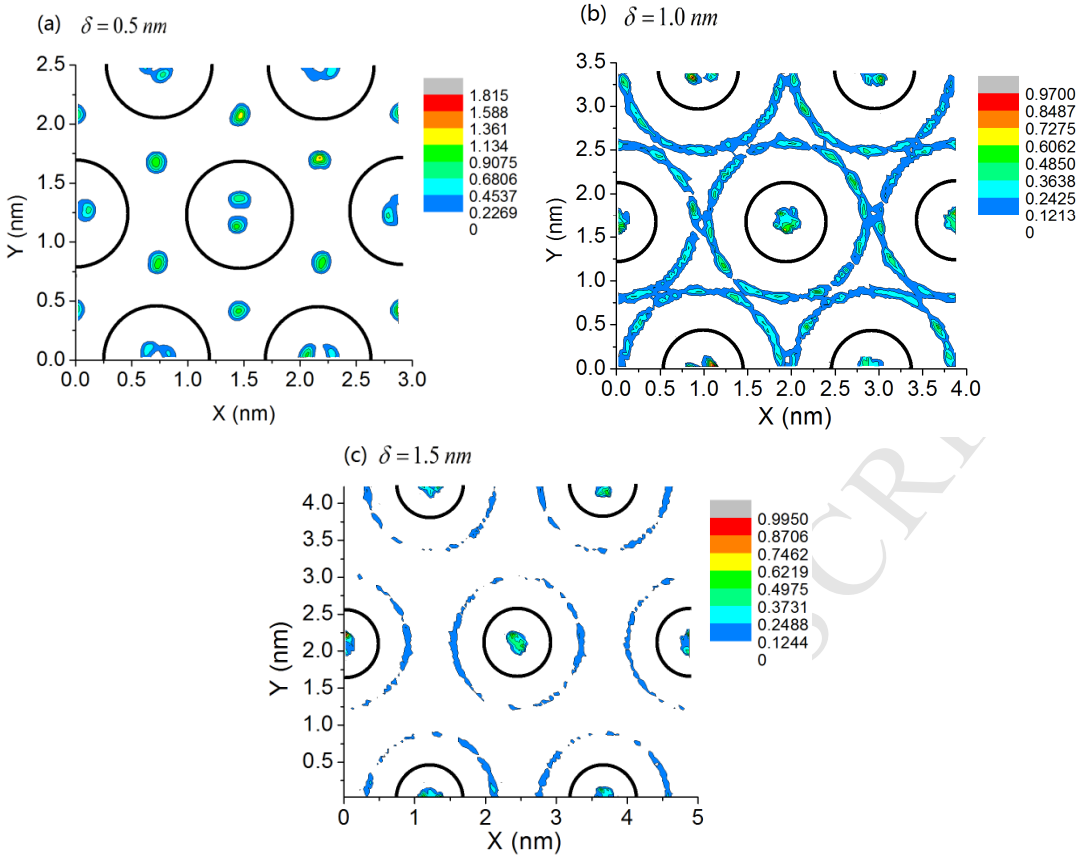

Figure 10. Density distributions at 10 bar and 300 K for CO_2 in (7, 7) CNT arrays carrying +0.05e charge, forh intertube distances of (a) 0.5 nm, (b) 1.0 nm and (c) 1.5 nm. The dark solid circles represent individual CNTs. The spacing used to map the density distributions is 0.05 nm in X and Y dimensions.

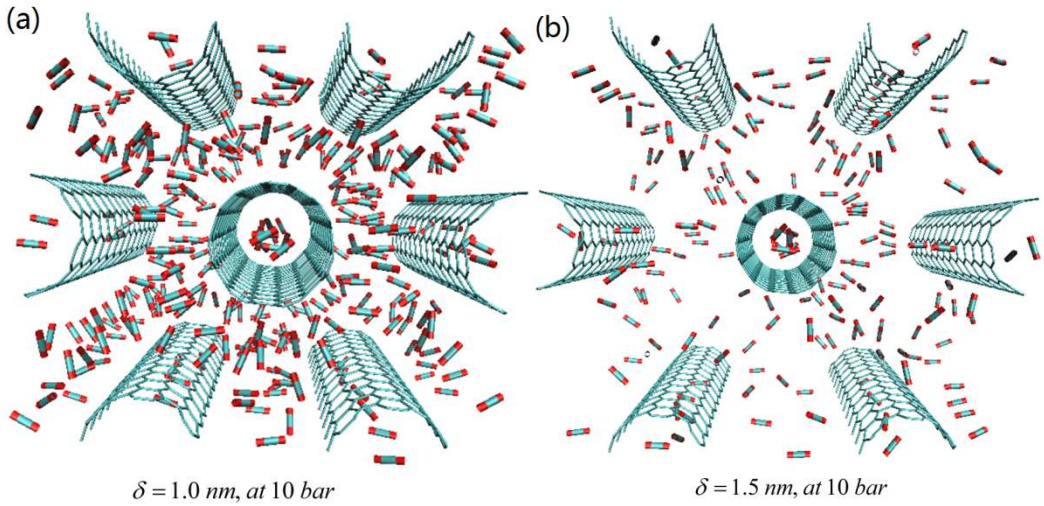

Figure 11. Snpashots of the configuration of CO_2 molecules adsorbed at 10 bar and 300 K in (7, 7) CNT arrays carrying +0.05e charge, and intertube separations of (a) 1.0 nm, (b) 1.5 nm. The red and cyan dots represent the oxygen and carbon atoms in the CO_2 molecule.

It is interesting to note (see Figure S7) that while the LJ interactions of adsorbate inside the CNT are almost constant when the intertube distance increases, the electrostatic interactions

are much weaker as intertube distance increases. Considering the rapid decay of the VDW interactions with the inter particle distance, it implies that the neighbouring CNTs apply negligible VDW interactions on the adsorption inside the tube, but strong electrostatic interactions facilitate/suppress the internal adsorption of CO_2/N_2 mixture in the charged CNTs. What is more important, the adsorbate-CNT electrostatic interactions for the adsorbate inside the CNT approach zero in the bundle with $\delta = 1.5$ nm, implying that while the surface charge from the neighbouring CNTs exerts strong electrostatic interactions on the adsorbate inside individual CNTs, the surface charge on the CNT that directly confines the adsorbate imposes negligible electrostatic interactions on the adsorbate. Thus the adsorption of a CO_2/N_2 mixture in an isolated CNT is expected to be insignificantly affected by the surface charge. Indeed, in our GCMC simulations we found the adsorption isotherms of pure CO_2 in the neutral and $\pm 0.1e$ charged (10, 10) CNTs at 300 K to be nearly identical, for pressures up to 15 bar. The CNT is located at the center of the simulation box, with dimension $L_x \times L_y \times L_z = 10 \times 10 \times 15$ nm^3, with periodic boundary conditions applied in all the dimensions. Accordingly, the orientation angles of CO_2 and N_2 inside the +0.05e charged tube generally decreases with the intertube distance as a result of reduced adsorbate-CNT electrostatic interactions. Table 3 lists the mean orientation angles of CO_2 adsorbed inside and outside the tube, which are averaged over all the internal and external molecules separately. In addition, the orientation angles inside the tube decrease with the pressure because the adsorbate-adsorbate interactions become more dominant at the high loadings, and the impact of adsorbate-host electrostatic interactions on orientation angle becomes weaker. On the other hand, as the adsorbate VDW interactions of with the CNT, for adsorbate located outside the CNT, decrease rapidly with the intertube distance, the electrostatic interactions first increase and then decrease with the intertube distance, and achieve a maximum at the intertube distance of 1.0 nm. Table 3 shows that the mean orientation angles of CO_2 and N_2 adsorbed in the interspace with an intertube distance of 1.0 nm are higher than those for other intertube separations. It is interesting to note that in the positively charged bundles with $\delta > 0.5\,nm$, the molecules adsorbed in the interspace distribute radially around each individual CNT, with the axis of each linear molecule pointing to the center of the central CNT. Figure 11 depicts the representative configurations of CO_2 adsorbed in the +0.05e positively charged (7, 7) CNT arrays with the intertube distances of 1.0 and 1.5 nm, at 10 bar. As confirmed in Figure 10 and Figure S7, molecules adsorbed in the grooves experience enhanced adsorbate-host electrostatic interactions as the axes of the adsorbate molecules are

parallel to the line connecting the centres of two opposite CNTs, with respect to adsorption in the interstices in the bundle with $\delta = 0.5$ nm. However, the electrostatic interactions of adsorbate-host are reduced as the intertube distance further increases from 1.0 to 1.5 nm. Consequently, the electrostatic interactions for the external adsorbate achieve the maximum in the bundle with $\delta = 1.0$ nm.

Table 3. Orientation angles of CO_2 and N_2 adsorbed inside the CNT and in the inter-space in the +0.05e charged (7, 7) CNT bundle at different pressures.

		angle θ (deg) inside			angle θ (deg) outside		
	intertube distance (nm)	1 bar	5 bar	15 bar	1 bar	5 bar	15 bar
CO_2	0.335	70.26	67.81	67.34			
	0.5	68.80	65.5	63.82	58.21	59.65	60.51
	1.0	64.09	61.09	59.91	73.20	71.02	69.28
	1.5	60.10	59.44	56.13	68.98	68.92	68.20
	0.335	65.50	65.15	65.97			
N_2	0.5	65.85	62.94	54.61	58.72	59.68	60.46
	1.0	61.67	62.36	57.94	62.65	61.72	62.16
	1.5	58.76	59.75	50.57	60.64	60.54	60.27

3.4 Effect of intertube distance on the performance of CNT bundles on CO_2 separation

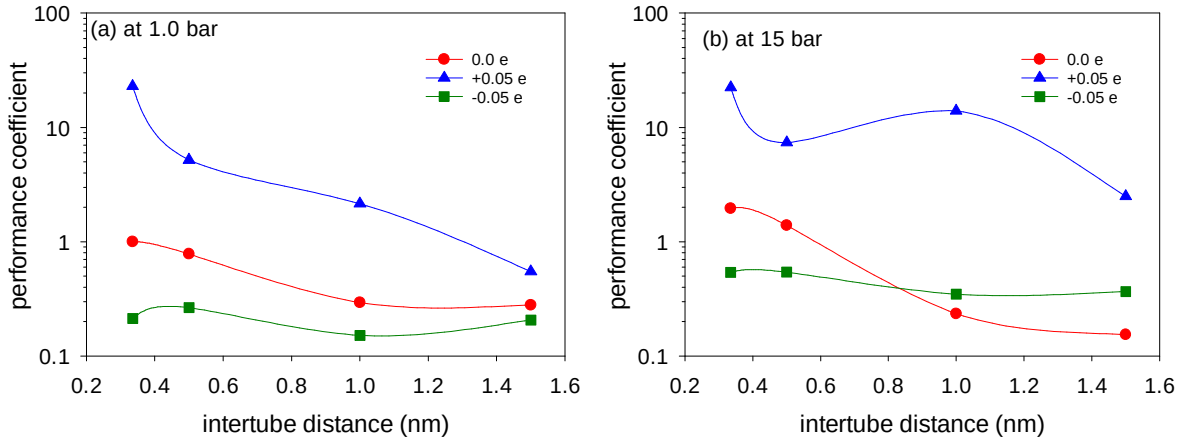

Figure 12. Performance coefficient at (a) 1.0 bar, and (b) 15 bar, at 300 K relative to a neutral CNT bundle with intertube separation of 0.335 nm at a pressure of 1.0 bar, for CO_2/N_2 (20/80) mixtures in ± 0.05 e charged CNT bundles with intertube separations ranging from 0.335 to 1.5 nm.

As demonstrated in Figure 8 and Figure S8, while the CO_2/N_2 selectivity generally decreases with the intertube distance in the neutral and ($\pm 0.05\,e$) charged bundles for intertube distances ranging from 0.335 to 1.5 nm, the adsorption of CO_2 demonstrates a complex dependency on the intertube distance. Therefore, to summarise the performance of bundles with different intertube distances, a coefficient that considers both adsorption and selectivity is required. We propose and employ the following performance coefficient λ_e,

$$\lambda_e = \exp\left[\ln\left(\alpha_1 \frac{M_t}{M_p} \right) + \ln\left(\alpha_2 \frac{S_t}{S_p} \right) \right] \tag{2}$$

based on the simulation data accumulated in this study. Here, M_t and M_p denote the gravimetric absolute adsorption of CO_2 in the target bundle at the target pressure, and the neutral bundle with $\delta = 0.335$ nm at 1.0 bar, respectively; S_t and S_p are the equilibrium selectivity of CO_2/N_2, and α_1 and α_2 are the weight factors, both set equal to 1.0. The plots in Figure 12, show that the performance of +0.05e charged CNT bundles with an intertube distance of 0.335 nm, is always superior to the neutral and negatively charged bundles, and that the performance generally decreases with the intertube distance. As an example, the +0.05e charged bundle with $\delta = 0.335$ nm is about 20 times better than that of a similar neutral bundle, whilst the -0.05e charged bundle is only about 20% of that of the neutral bundle. The large difference between the positively and negatively charged bundles, suggests that charged CNT bundles are a very promising material for use in electric swing adsorption for the capture of CO_2 from flue gas [3, 20]. Since there is an even greater discrepancy between the electrostatic properties of CO_2 and CH_4, the application of charged CNT bundles to separate CO_2 from natural gas is a promising subject for future study [6].

Figures 12 (a) and (b), demonstrate that increasing the pressure improves the performance of the CNT bundles, mainly because more CO_2 is adsorbed at higher pressures. However, in the neutral CNT bundle, when the intertube distance is above 0.5 nm, increasing the pressure from 1.0 to 15 bar reduces the performance as there is a significant reduction in the CO_2/N_2 selectivity, (see Figures S8 (a) and (b)). At 15 bar in the +0.05e charged bundle with $\delta = 1.0$ nm, the performance coefficient is higher than that in the bundle with $\delta = 0.5$ nm, which may be attributed to the greatly enhanced adsorption of CO_2 in the inter-space, as a consequence of the strong CO_2-CNT electrostatic interactions in the grooves. Intriguingly, the performance of -0.05e charged CNT bundles with an intertube distance larger than 0.5 nm exceeds that of

neutral bundles with the same intertube distances at high pressure. Our simulations show that, although the negative charges suppress the adsorption of CO_2 inside the CNT, they impose noticeable attractive electrostatic interactions on the CO_2 molecules but repulsive or very weak attractive electrostatic interactions on N_2 molecules located in the interstices and the groove space, favouring the adsorption of CO_2 in the interspace, evident in Figure S9 (b). Additionally, as shown in Figure S9 (a), the CO_2-CNT VDWs interactions for CO_2 located in the interspace of the -0.05e charged CNT bundles are also slightly greater than those in the neutral CNT bundles. Unlike the distribution of CO_2 molecules in the positively charged CNT bundles, CO_2 molecules adsorbed in the interspace of the negatively charged bundles distribute around individual CNTs with the axis of the CO_2 molecule tangential to a line connecting the center of mass of CO_2 and the center of the CNT. Further, in the absence of surface charge, CO_2 molecules located in the interspace distribute around the CNT with random orientation angles in the neutral CNT bundles, (Figure S10). As a consequence, the enhancement in the adsorption of CO_2 in the interspace contributed by the negative surface charge overcomes the reduction in the adsorption of CO_2 in the internal space at high pressure, at which the adsorption of CO_2 in the interspace becomes comparable to or dominant over the adsorption inside the tube. In this case, the performance of -0.05e charged CNT bundles with an intertube distance larger than 0.5 nm, exceeds that of neutral CNT bundles with the same intertube distance at the high pressure.

However, since flue gases are generally saturated with water, it is essential to understand the role of water vapor on the performance of (7, 7) CNT bundles in separating CO_2 from flue gas. We depict the adsorption isotherms of each component and the CO_2/N_2 selectivities for the ternary mixture $CO_2/N_2/H_2O$ saturated with water (bulk composition is CO_2:N_2=20:80 with H_2O at its saturation pressure) in neutral and charged (7, 7) CNT bundles with intertube separation of 0.335 nm, in Figure S11. It can be seen the adsorption of H_2O is always negligible compared to that of CO_2 in the neutral and positively charged (7, 7) CNT bundles, and the effect of water vapor in the gas phase on the CO_2/N_2 selectivity is subsequently negligible. However, when the negative surface charge is above -0.01e, with the adsorption CO_2 being suppressed by the negative surface charge, H_2O adsorbs into the negatively charged CNT and completely takes over the adsorption space, leading to negligible adsorption of CO_2 and N_2 in the CNT bundles. It is interesting to note that in the CNT bundle carrying -0.01e charge in which the suppression effect of the negative surface charge on the adsorption of CO_2 becomes less prevalent, the adsorption of H_2O is dominant at the low

pressure and then reduces significantly with pressure. This is because with increasing the pressure, the partial pressures of CO_2 and N_2 become much higher than that of saturated water vapor in the gas phase, leading to the adsorption of CO_2 and N_2 becomes dominant at the high pressure. Nevertheless, without the suppression effect from the negative surface charge, the adsorption of CO_2 in the neutral and positively charged CNT bundles is always preferable over the H_2O and N_2, severely restricting the adsorption of H_2O and N_2. Indeed, the H_2O-host interactions including the (LJ and coulomb parts) are quite comparable in the -0.05e and +0.05e charged CNT bundles, which are -35.6 and -31.5 kJ/mol respectively, and both of which are significant higher than that in the neutral CNT bundle, -12.4 kJ/mol. Therefore, the strong adsorption of H_2O in the negatively charged CNT bundles is a result of reduced adsorption of CO_2 and additional H_2O-CNT electrostatic interactions, and the negligible adsorption of H_2O in the positively charged CNT bundles is a consequence of competition between the dominant adsorption of CO_2 and restricted adsorption of H_2O. The negligible adsorption of water vapor in the neutral CNT bundle is simply because of the hydrophobicity of the CNT wall, exerting weak interactions on H_2O [43]. In conclusion, water vapor existing in the flue gas only applies insignificant effect on the optimized performance of (7, 7) CNT bundles in separating CO_2 from flue gas. However, dehydration is needed for the negatively charged CNT bundles prior to the electric swing adsorption procedure.

4 Conclusions

The adsorption of CO_2/N_2 mixtures (20/80 in the gas phase) at 300 K, in neutral and charged hexagonal (7, 7) CNT arrays with intertube distances ranging from 0.335 to 1.5 nm, and pressures up to 15 bar, has been investigated. Surface charges of $0.0, \pm 0.01, \pm 0.02$ and $\pm 0.05e$ were assigned to each carbon atom. It was found that a positive charge on the CNT bundles enhances the adsorption of CO_2 and the CO_2/N_2 selectivity, while negative charges suppress the adsorption and the selectivity for CO_2, compared to those in the neutral CNT bundle. At atmospheric pressure and ambient temperature, the CO_2/N_2 selectivity in the +0.05e charged (7, 7) CNT bundle with an intertube distance of 0.335 nm exceeds 1000, and is superior to a wide range of nanoporous materials including MOFs, ZIFs, zeolites and activated carbons, summarised in Table 2. While increasing the positive charge increases both the mean orientation angle of the adsorbate and the adsorbate-CNT interaction inside the

CNT, increasing the negative charge reduces the orientation angle of the adsorbate whilst the CO_2-CNT interactions are almost unaffected. The reduced adsorption of CO_2 in the negatively charged CNT bundles can be attributed to the reduction in the available adsorption volume with a consequent decrease in entropy for CO_2 molecules. Conversely, in the positively charged system, both N_2 and CO_2 tend to span the pores to enable the negative charges at each end of the molecular axis to benefit from electrostatic interaction with the surface charge, favouring the adsorption of CO_2 and thus leaving limited adsorption space for N_2.

Increasing the intertube distance can either enhance or reduce the adsorption of CO_2, depending on the competition between the additional adsorption volume in the intertube space and the reduced adsorbate-CNT interactions for the adsorbate inside and outside the CNT. However, the CO_2/N_2 selectivity decreases monotonically with intertube distance in the charged and neutral CNT bundles, due to the reduction in the adsorbate-CNT interactions. Upon increasing the intertube distance, the favourable adsorption in the intertube space shifts from the interstices to the grooves. Nevertheless, the space inside the CNT is always more favourable for the adsorption of CO_2 compared to the interstices and the grooves in the positively charged (7, 7) CNT bundles. We show that the electrostatic interactions from the neighbouring CNTs account for the enhanced adsorption of CO_2 inside the CNT in the positively charged CNT bundles, indicating negligible electrostatic interactions of adsorbate with the CNT that confines the adsorbate inside. When the CNT separation is sufficiently large to permit CO_2 molecules to occupy the intertube space, molecules adsorbed outside the CNT distribute radially around the CNT with the axes of the molecules pointing to the center of the positively charged CNT, and tangential to the periphery for the negatively charged CNT.

The performance of CNT bundles has been summarised in a simple equation, treating the adsorption capacity and the selectivity as equally important; we find that increasing the pressure generally improves performance, while increasing the intertube distance reduces it. From the comprehensive calculations presented here we find that the +0.05e charged (7, 7) CNT bundle with an intertube distance of 0.335 nm provides the best performance in separating CO_2, for pressure up to 15 bar. Essentially, it is found that moisture in the flue gas imposes negligible effect on the optimal performance of (7, 7) CNT bundles on CO_2 separation from flue gas.

Acknowledgement

This work has been supported by a grant from the Australian Research Council through the Discovery scheme (Grant No. DP150101824). This research was undertaken with the assistance of the computational resources provided at the NCI National Facility systems at the Australian National University (ANU), and those at the Pawsey Supercomputing Centre in Western Australia, through their National Computational Merit Allocation Schemes supported by the Australian Government and the Government of Western Australia.

Supplementary Material

Figures showing adsorption isotherms of CO_2/N_2 mixture in amorphous carbon, SiC-DC, effects of the LJ interaction strength on the adsorption of CO_2/N_2 mixture in CNT bundles, effect of charge on adsorbate orientation and density profiles, variation of electrostatic and van Der Waals interaction energy with intertube spacing, adsorption isotherms, and snapshots of configurations for different intertube spacings and charges, adsorption isotherms of ternary $CO_2/N_2/H_2O$ mixtures saturated with water in the neutral and charged (7, 7) CNT bundles are given in the Supplementary Material.

References

[1] M.Z. Jacobson, Review of solutions to global warming, air pollution, and energy security, Energy Environ. Sci. 2 (2) (2009) 148-173.

[2] D. Aaron, C. Tsouris, Separation of CO_2 from flue gas: a review, Separ. Sci. Technol. 40 (1-3) (2005) 321-348.

[3] C.A. Grande, A.E. Rodrigues, Electric swing adsorption for CO_2 removal from flue gases, Int. J. Greenh. Gas. Con. 2 (2) (2008) 194-202.

[4] M. Romero-Hermida, J.M. Romero-Enrique, V. Morales-Flórez, L. Esquivias, Flue gas adsorption by single-wall carbon nanotubes: A Monte Carlo study, The J. Chem. Phys. 145(7) (2016) 074701-1-074701-14.

[5] S. Iijima, Helical microtubules of graphitic carbon, Nature 354 (6348) (1991) 56-58.

[6] L. Liu, D. Nicholson, S.K. Bhatia, Adsorption of CH_4 and CH_4/CO_2 mixtures in carbon nanotubes and disordered carbons: a molecular simulation study, Chem. Eng. Sci. 121 (2015) 268-278.

[7] A.I. Skoulidas, D.M. Ackerman, J.K. Johnson, D.S. Sholl, Rapid transport of gases in carbon nanotubes, Phys. Rev. Lett. 89 (18) (2002) 185901.

[8] P. Kowalczyk, S. Furmaniak, P.A. Gauden, A.P. Terzyk, Optimal single-walled carbon nanotube vessels for short-term reversible storage of carbon dioxide at ambient temperatures, J. Phys. Chem. C 114 (49) (2010) 21465-21473.

[9] A.R. Millward, O.M. Yaghi, Metal-organic frameworks with exceptionally high capacity for storage of carbon dioxide at room temperature, J. Am. Chem. Soc. 127 (51) (2005) 17998-17999.

[10] R. Babarao, J. Jiang, Unprecedentedly high selective adsorption of gas mixtures in rho zeolite-like metal−organic framework: a molecular simulation study, J. Am. Chem. Soc. 131 (32) (2009) 11417-11425.

[11] B. Liu, B. Smit, Molecular simulation studies of separation of CO_2/N_2, CO_2/CH_4, and CH_4/N_2 by ZIFs, J. Phys. Chem. C 114 (18) (2010) 8515-8522.

[12] H. Fang, A. Kulkarni, P. Kamakoti, R. Awati, P.I. Ravikovitch, D.S. Sholl, Identification of high CO_2 capacity cationic zeolites by accurate computational screening, Chem. Mater. 28(11) (2016) 3887-3896.

[13] D.M. D'Alessandro, B. Smit, J.R. Long, Carbon dioxide capture: prospects for new materials, Angew. Chem. Int. Edit. 49 (35) (2010) 6058-6082.

[14] G. Gao, T. Çağin, W.A. Goddard, Position of K atoms in doped single-salled carbon nanotube crystals, Phys. Rev. Lett. 80 (25) (1998) 5556-5559.

[15] R.S. Lee, H.J. Kim, J.E. Fischer, A. Thess, R.E. Smalley, Conductivity enhancement in single-walled carbon nanotube bundles doped with K and Br, Nature 388 (6639) (1997) 255-257.

[16] W.-Q. Deng, X. Xu, W.A. Goddard, New alkali doped pillared carbon materials designed to achieve practical reversible hydrogen storage for transportation, Phys. Rev. Lett. 92 (16) (2004) 166103.

[17] H. Pan, J. Li, Y. Feng, Carbon nanotubes for supercapacitor, Nanoscale Res. Lett. 5 (3) (2010) 654-668.

[18] R. Stoian, A. Rosenfeld, D. Ashkenasi, I.V. Hertel, N.M. Bulgakova, E.E.B. Campbell, Surface charging and impulsive ion ejection during ultrashort pulsed laser ablation, Phys. Rev. Lett. 88 (9) (2002) 097603-1-097603-4.

[19] M. Zdrojek, T. Mélin, H. Diesinger, D. Stiévenard, W. Gebicki, L. Adamowicz, Charging and discharging processes of carbon nanotubes probed by electrostatic force microscopy, J. Appl. Phys. 100 (11) (2006) 114326-1-114326-10.

[20] M. Rahimi, J.K. Singh, F. Müller-Plathe, CO_2 Adsorption on charged carbon nanotube arrays: a possible functional material for electric swing adsorption, J. Phys. Chem. C 119 (27) (2015) 15232-15239.

[21] V.V. Simonyan, P. Diep, J.K. Johnson, Molecular simulation of hydrogen adsorption in charged single-walled carbon nanotubes, J. Chem. Phys. 111 (21) (1999) 9778-9783.

[22] W.A. Steele, The interaction of rare gas atoms with graphitized carbon black, J. Phys. Chem. 82 (7) (1978) 817-821.

[23] J.G. Harris, K.H. Yung, Carbon dioxide's liquid-vapor coexistence curve and critical properties as predicted by a simple molecular model, J. Phys. Chem. 99 (31) (1995) 12021-12024.

[24] J.J. Potoff, J.I. Siepmann, Vapor–liquid equilibria of mixtures containing alkanes, carbon dioxide, and nitrogen, AIChE J. 47 (7) (2001) 1676-1682.

[25] M.P. Allen, D.J. Tildesley, Computer simulation of liquids, Oxford University Press, Oxford, 1989.

[26] O. Kunz, W. Wagner, The gerg-2008 wide-range equation of state for natural gases and other mixtures: an expansion of gerg-2004, J. Chem. Eng. Data 57 (11) (2012) 3032-3091.

[27] S.S. Razavi, S.M. Hashemianzadeh, H. Karimi, Modeling the adsorptive selectivity of carbon nanotubes for effective separation of CO_2/N_2 mixtures, J. Mol. Model. 17(5) (2011) 1163-1172.

[28] R.F. Cracknell, D. Nicholson, S.R. Tennison, J. Bromhead, Adsorption and selectivity of carbon dioxide with methane and nitrogen in slit-shaped carbonaceous micropores: simulation and experiment, Adsorption 2 (3) (1996) 193-203.

[29] T.X. Nguyen, N. Cohaut, J.-S. Bae, S.K. Bhatia, New method for atomistic modeling of the microstructure of activated carbons using hybrid reverse Monte Carlo simulation, Langmuir 24 (15) (2008) 7912-7922.

[30] A.H. Farmahini, G. Opletal, S.K. Bhatia, Structural modelling of silicon carbide-derived nanoporous carbon by hybrid reverse Monte Carlo simulation, J. Phys. Chem. C 117 (27) (2013) 14081-14094.

[31] Q. Yang, C. Xue, C. Zhong, J.F. Chen, Molecular simulation of separation of CO_2 from flue gases in Cu-BTC metal-organic framework, AIChE J. 53 (11) (2007) 2832-2840.

[32] A. Martín-Calvo, E. García-Pérez, J. Manuel Castillo, S. Calero, Molecular simulations for adsorption and separation of natural gas in IRMOF-1 and Cu-BTC metal-organic frameworks, Phys. Chem. Chem. Phys. 10 (47) (2008) 7085-7091.

[33] L. Bastin, P.S. Bárcia, E.J. Hurtado, J.A.C. Silva, A.E. Rodrigues, B. Chen, A microporous metal organic framework for separation of CO_2/N_2 and CO_2/CH_4 by fixed-bed adsorption, J. Phys. Chem. C 112 (5) (2008) 1575-1581.

[34] R. Krishna, J.M. van Baten, A comparison of the CO_2 capture characteristics of zeolites and metal–organic frameworks, Sep. Purif. Technol. 87 (2012) 120-126.

[35] A. Goj, D.S. Sholl, E.D. Akten, D. Kohen, Atomistic simulations of CO_2 and N_2 adsorption in silica zeolites: the impact of pore size and shape, J. Phys. Chem. B 106 (33) (2002) 8367-8375.

[36] R. Krishna, J.M. van Baten, Comment on comparative molecular simulation study of CO_2/N_2 and CO_2/CH_4 separation in zeolites and metal−organic frameworks, Langmuir 26 (4) (2010) 2975-2978.

[37] E.D. Akten, R. Siriwardane, D.S. Sholl, Monte Carlo simulation of single- and binary-component adsorption of CO_2, N_2, and H_2 in zeolite Na-4A, Energ Fuel 17 (4) (2003) 977-983.

[38] J. Jiang, S.I. Sandler, Separation of CO_2 and N_2 by adsorption in C168 Schwarzite: A combination of quantum mechanics and molecular simulation study, J. Am. Chem. Soc. 127(34) (2005) 11989-11997.

[39] F. Su, C. Lu, W. Cnen, H. Bai, J.F. Hwang, Capture of CO_2 from flue gas via multiwalled carbon nanotubes, Sci. Total. Environ. 407(8) (2009) 3017-23.

[40] L. Wang, R.T. Yang, Significantly increased CO_2 adsorption performance of nanostructured templated carbon by tuning surface area and nitrogen doping, J. Phys. Chem. C 116(1) (2012) 1099-1106.

[41] A.J. Du, C.H. Sun, Z.H. Zhu, G.Q. Lu, V. Rudolph, C.S. Sean, The effect of Fe doping on adsorption of CO_2 /N_2 within carbon nanotubes: a density functional theory study with dispersion corrections, Nanotechnology 20(37) (2009) 375701-1-375701-4.

[42] J.-C. Charlier, Defects in carbon nanotubes, Acc. Chem. Res. 35(12) (2002) 1063-1069.

[43] L. Liu, D. Nicholson, S.K. Bhatia, Impact of H_2O on CO_2 separation from natural gas: comparison of carbon nanotubes and disordered carbon, J. Phys. Chem. C 119(1) (2014) 407-419.